PHYSICAL REVIEW B VOLUME 1, NUMBER 12 15 JUNE 1970

# Theory of Metal Surfaces: Charge Density and Surface Energy*

N. D. Lang† and W. Kohn
*Department of Physics, University of California, San Diego, La Jolla, California* 92037
(Received 28 January 1970)

The first part of this paper deals with the jellium model of a metal surface. The theory of the inhomogeneous electron gas, with local exchange and correlation energies, is used. Self-consistent electron density distributions are obtained. The surface energy is found to be negative for high densities ($r_s \leq 2.5$). In the second part, two corrections to the surface energy are calculated which arise when the positive background model is replaced by a pseudopotential model of the ions. One correction is a cleavage energy of a classical neutralized lattice, the other an interaction energy of the pseudopotentials with the electrons. Both of these corrections are essential at higher densities ($r_s \leq 4$). The resulting surface energy is in semiquantitative agreement with surface-tension measurements for eight simple metals (Li, Na, K, Rb, Cs, Mg, Zn, Al), typical errors being about 25%. For Pb there is a serious disagreement.

## I. INTRODUCTION

The electron theory of metals has always been primarily concerned with properties of the metal interior. These bulk properties are, of course, of great fundamental interest, and, fortunately for the theorist, the translational invariance prevailing inside the metal introduces important elements of simplicity into calculations. In the last 10–15 years there has been excellent progress in the treatments of both electron-ion and electron-electron interactions, so that bulk theories are now capable of giving quantitatively accurate descriptions of wide classes of metals.[1-3]

Theories of metal surfaces have, relatively speaking, lagged far behind. This has been due primarily to the great additional difficulties produced by the rapid decrease of electron density near the surface and by the loss of translational symmetry. After an early work by Frenkel,[4] there was an important paper by Bardeen[5] who performed an approximately self-consistent calculation for Na. During the following three decades, there were very few theoretical attempts on the metal surface problem.[6] Quite recently, a new general formulation of electron theory, expressly devised to deal with systems of inhomogeneous electron density, was put forward by Hohenberg, Kohn, and Sham.[7,8] This formulation has been used in several new investigations of the electronic structure of metal surfaces. Bennett and Duke[9] and Smith[10] have performed approximately self-consistent calculations, using this theory, for a popular model of the metal surface in which the ions are replaced by a uniform semi-infinite positive charge density. A fully self-consistent calculation along the same lines has been reported briefly by one of the present authors.[11] These studies give, for the work function, good qualitative agreement with experiment over a wide range of densities. The calculated surface energy, however, while in fair agreement with experiment at low electron densities, fails completely – to the point of giving the wrong sign – for higher-density metals such as Al.

The present paper is aimed particularly at the problem of the surface energy. In Sec. II, we describe a fully self-consistent calculation for the uniform background (or jellium) model of a metal surface, using the theory of Refs. 7 and 8. Numerical results for density distributions (including Friedel oscillations), potentials, and surface energies are presented for the full range of metallic densities.[12]

However, as already remarked, the uniform background model is totally inadequate for describing the surface energy of high-density metals. In Sec. III, we supplement this model by first-order pseudopotential calculations (using the zero-order density distributions of the uniform background model) and by the addition of the appropriate electrostatic lattice energies. The resulting surface energies are found to be in rather good agreement with experiment over the entire range of metallic densities.

In a subsequent paper we shall describe the effects of the ionic lattice on the work function, particularly on the anisotropies associated with different crystal faces.

## II. UNIFORM POSITIVE BACKGROUND MODEL

### A. Mathematical Formulation

We address ourselves to the problem of determining the surface electronic structure in the model of a metal in which the positive charges are replaced by a uniform charge background of density

$$n_+(\vec{r}) = \bar{n}, \quad x \leq 0$$
$$= 0, \quad x > 0. \tag{2.1}$$

For orientation, we remark that a Thomas-Fermi calculation[13,14] leads to an electron density distribution which decreases smoothly from its interior value $\bar{n}$ to zero, over a distance of the order of the Thomas-Fermi screening length [see Fig. 1(a)]. However, for quantitative purposes, such a calculation is quite inadequate. It leads to a vanishing work function and negative surface energies, and does not exhibit the important Friedel oscillations of the electron density near the surface.

The analysis presented here uses the self-consistent equations of Kohn and Sham.[8] These are based on the general theory of the inhomogenous electron gas,[7] which includes exchange and correlation effects. We review these equations here briefly.

It is shown in Refs. 7 and 8 that the total electronic ground-state energy of a many-electron system in an external potential $v(\vec{r})$ can be written in the following form[15]:

$$E_v[n] = \int v(\vec{r})\, n(\vec{r})\, d\vec{r} + \tfrac{1}{2} \int \frac{n(\vec{r})\, n(\vec{r}')}{|\vec{r} - \vec{r}'|}\, d\vec{r} d\vec{r}' + T_s[n] + E_{xc}[n] \,. \tag{2.2}$$

Here the functional $T_s[n]$ is the kinetic energy of a noninteracting electron system of density distribution $n(\vec{r})$, and the functional $E_{xc}[n]$ represents the exchange and correlation energy (Hartree theory corresponds to setting $E_{xc} \equiv 0$). One then defines an effective potential

$$v_{\text{eff}}[n; \vec{r}] = v(\vec{r}) + \int \frac{n(\vec{r}')}{|\vec{r} - \vec{r}'|}\, dr' + v_{xc}[n; \vec{r}], \tag{2.3}$$

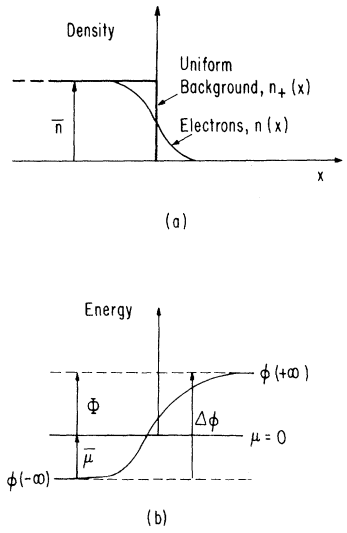


FIG. 1. Schematic representation of (a) density distributions and (b) various energies relevant to the metal surface problem.

where $v_{xc}[n; \vec{r}] \equiv \dfrac{\delta E_{xc}[n]}{\delta n(\vec{r})}$ . (2.4)

Assuming that the form of $E_{xc}[n]$ and hence of $v_{\text{eff}}[n; \vec{r}]$ is known, the solution of the following self-consistency problem gives the exact density distribution of the system of $N$ interacting electrons:

$$\{-\tfrac{1}{2}\nabla^2 + v_{\text{eff}}[n; \vec{r}]\}\, \psi_i = \epsilon_i \psi_i \,, \tag{2.5a}$$

$$n(\vec{r}) = \sum_{i=1}^{N} |\psi_i(\vec{r})|^2 \,, \tag{2.5b}$$

where the $\psi_i$ are the $N$ lowest-lying orthonormal solutions of (2.5a). The energy $E_v[n]$ of the system is given by (2.2), with

$$T_s[n] = \sum_{i=1}^{N} \epsilon_i - \int v_{\text{eff}}[n; \vec{r}]\, n(\vec{r})\, d\vec{r} \,. \tag{2.6}$$

It is convenient at this point to state a number of facts [Eqs. (2.7)–(2.12)] which are strictly correct for the present model [Eq. (2.1)], including all many-body effects. Some of these statements are illustrated in Fig. 1.

The electrostatic potential energy difference of an electron between $x = +\infty$ and $x = -\infty$, the so-called electrostatic dipole barrier, which we denote by $\Delta\varphi$, is given by

$$\Delta\varphi \equiv \varphi(+\infty) - \varphi(-\infty)$$
$$= 4\pi \int_{-\infty}^{\infty} dx \int_{x}^{\infty} dx' \,[n(x') - n_+(x')]$$
$$= 4\pi \int_{-\infty}^{\infty} x[n(x) - n_+(x)]\, dx \,. \tag{2.7}$$

The chemical potential $\mu$ of this system, defined, as usual, as the ground-state energy difference of the $N+1$ and $N$ electron systems (with the background charge fixed at $N|e|$) is given by

$$\mu = \varphi(-\infty) + \bar{\mu} \,, \tag{2.8a}$$

where $\bar{\mu}$ is the intrinsic chemical potential of the infinite system (relative to the electrostatic potential in this system).[16] From its definition, $\bar{\mu}$ is given by

$$\bar{\mu} = \tfrac{1}{2} k_F^2 + \left(\frac{\delta E_{xc}[n]}{\delta n}\right)_{n=\bar{n}} \equiv \tfrac{1}{2} k_F^2 + \mu_{xc}(\bar{n}) \,, \tag{2.8b}$$

where $k_F$ is the Fermi momentum of a degenerate electron gas of density $\bar{n}$ and $\mu_{xc}(n)$ is the exchange and correlation part of the chemical potential of an infinite uniform electron gas of density $n$. If the exchange and correlation energy per particle of such a gas is denoted by $\epsilon_{xc}(n)$, then from the definition of $E_{xc}[n]$,

$$\mu_{xc}(n) = \frac{d}{dn}\,(n\epsilon_{xc}(n)) \,. \tag{2.8c}$$

The work function, defined as the minimum energy necessary to eject an electron, is[17]

$$\Phi = \varphi(+\infty) - \mu = \Delta\varphi - \bar{\mu} \ . \qquad (2.9)$$

In the interior of the metal, $v_{eff}$ approaches a constant value [see (2.3), (2.4), and (2.8c)]:

$$v_{eff} \to \varphi(-\infty) + \mu_{xc}(\bar{n}) \ . \qquad (2.10)$$

Hence the eigenfunctions of (2.5a) can be labeled by the quantum numbers $k$, $k_y$, $k_z$, with the following meaning:

$$\psi_{k,\,k_y,\,k_z} = \psi_k(x)\exp[i(k_y y + k_z z)] \ , \qquad (2.11a)$$

where, for $x \to -\infty$,

$$\psi_k(x) = \sin[kx - \gamma(k)] \ . \qquad (2.11b)$$

Here $\gamma(k)$ is the phase shift which is uniquely determined by the conditions that $\gamma(0) = 0$ and that $\gamma(k)$ be continuous. The eigenvalues of (2.5a) are then [from (2.10)]

$$\epsilon_{k,\,k_y,\,k_z} = \varphi(-\infty) + \mu_{xc}(\bar{n}) + \tfrac{1}{2}(k^2 + k_y^2 + k_z^2) \ . \qquad (2.12a)$$

If for convenience we choose the zero of energy so that

$$\mu = 0 \ , \qquad (2.13)$$

then by (2.8), $\varphi(-\infty) + \mu_{xc}(\bar{n}) = -\tfrac{1}{2}k_F^2$, and (2.12a) becomes

$$\epsilon_{k,\,k_y,\,k_z} = \tfrac{1}{2}(k^2 + k_y^2 + k_z^2 - k_F^2) \ . \qquad (2.12b)$$

In order now to make practical use of the theory embodied in Eqs. (2.2)–(2.6), some approximate form of the exchange and correlation energy functional is required. For a system with very slowly varying density, we have

$$E_{xc}[n] = \int \epsilon_{xc}(n(\vec{r}))\, n(\vec{r})\, d\vec{r} \ , \qquad (2.14)$$

with errors proportional to the squares of the density gradients.[5] Following Refs. 8 and 18, we shall use this form for the present problem, even though in the surface region of a typical metal the density varies quite rapidly. A "control" calculation, to be described below, and the fact that the final results are in rather good agreement with experiment suggest that the errors introduced by approximation (2.14) are not too serious. This question is discussed again later on in the present section, and in the concluding remarks.

For $\epsilon_{xc}(n)$, the exchange and correlation energy per particle of a uniform electron gas, we use the approximation due to Wigner.[19] In atomic units, it is

$$\epsilon_{xc}(n) = -\frac{0.458}{r_s(n)} - \frac{0.44}{r_s(n) + 7.8} \ , \qquad (2.15a)$$

where $r_s(n)$ is defined by

$$(4\pi/3)[r_s(n)]^3 = 1/n \ . \qquad (2.15b)$$

Other more recently suggested forms of the correlation energy[20] give, within a few percent, the same results.

We can now rewrite the self-consistency problem (2.5) in a form specific to the present problem:

$$\left\{-\frac{1}{2}\frac{d^2}{dx^2} + v_{eff}[n;\ x]\right\}\psi_k(x) = \tfrac{1}{2}(k^2 - k_F^2)\,\psi_k(x) \ , \qquad (2.16a)$$

where $\psi_k$ has the asymptotic form (2.11b). $v_{eff}$ is given by

$$v_{eff}[n;x] = \Phi[n] - 4\pi\int_x^\infty dx' \int_{x'}^\infty dx'' \times [n(x'') - n_+(x'')] + \mu_{xc}(n(x)) \ , \qquad (2.16b)$$

with $\Phi[n] = \Delta\varphi[n] - \bar{\mu}$ . (2.16c)

The density is in turn given by

$$n(x) = \frac{1}{\pi^2}\int_0^{k_F} (k_F^2 - k^2)[\psi_k(x)]^2\, dk \ . \qquad (2.16d)$$

The numerical solution of these equations requires careful treatment of quantum oscillations which are present in the density and potential (see Appendix A 1). Details concerning the method of solution are given in Appendix B.

### B. Density Distributions and Potentials

The self-consistent system of Eqs. (2.16) was solved for the bulk metallic density range $r_s = 2 - 6$ at intervals of 0.5. The degree of self-consistency achieved in $n(x)$ varied from 0.08% (for $r_s = 2$) to 0.7% (for $r_s = 6$) of the asymptotic density $\bar{n}$.

Table I gives $n(x)$ for $r_s = 2,\ 3,\ \ldots\ 6$, and Fig. 2 displays $n(x)$ for $r_s = 2$ and 5. It will be observed that for the low mean density corresponding to $r_s = 5$, there are sizeable Friedel oscillations, including an overshoot of $\bar{n}$ by 12%. On the other hand, at the high mean density corresponding to $r_s = 2$, the density distribution begins to resemble the monotonically decreasing form of the Thomas-Fermi theory (cf. discussion in Appendix A 2).

Figure 3 shows the electrostatic potential energy $\varphi(x)$ and the effective potential $v_{eff}[n;\ x]$ for $r_s = 5$. It will be noticed that the electrostatic barrier $\Delta\varphi = \varphi(\infty) - \varphi(-\infty)$ is very small, but that in the vicinity of the surface, $\varphi(x)$ exhibits substantial oscillation. The corresponding oscillation in $v_{eff}$ is considerably smaller. This can be explained by the fact that, for large negative $x$, the oscillatory terms of $\varphi$ and of the exchange part of $\mu_{xc}$ cancel exactly (Appendix A). Both $\varphi$ and $v_{eff}$ are given in Table I for integral $r_s$ values from 2 to 6.

Approximation (2.14) for $E_{xc}[n]$ is based on the assumption of a nearly uniform gas. It leads to an effective exchange and correlation potential

TABLE I. Electron density $n(x)$ in units of $\bar{n}$ (the interior density), and the effective potential $v_{\rm eff}(x)$, and electrostatic potential $\varphi(x)$, in units of $\frac{1}{2}k_F^2$. The distance $x$ from the surface of the positive background is given in units of $2\pi/k_F$, the Fermi wavelength. $r_s$, the usual Wigner-Seitz radius for an electron, characterizes the interior density. Entries in the Table are given to four decimal places so as to better characterized the Freidel oscillations, even though the density, for example, is only self-consistent to between 0.08%($r_s=2$) and 0.7%($r_s=6$) of $\bar{n}$. As $x\to\infty$, $n(x)$ tends exponentially to 0, while the potentials both tend exponentially to the work function $\Phi$ (though $v_{\rm eff}$ approaches this limit more slowly than $\varphi$).

| $x$ | $r_s=2$ | | | $r_s=3$ | | | $r_s=4$ | | | $r_s=5$ | | | $r_s=6$ | | |
|---|---|---|---|---|---|---|---|---|---|---|---|---|---|---|---|
| | $n(x)$ | $v_{\rm eff}(x)$ | $\varphi(x)$ | $n(x)$ | $v_{\rm eff}(x)$ | $\varphi(x)$ | $n(x)$ | $v_{\rm eff}(x)$ | $\varphi(x)$ | $n(x)$ | $v_{\rm eff}(x)$ | $\varphi(x)$ | $n(x)$ | $v_{\rm eff}(x)$ | $\varphi(x)$ |
| -1.200 | 1.0036 | -1.0000 | -0.2316 | 1.0037 | -1.0004 | 0.2135 | 1.0031 | -1.0013 | 0.6876 | 1.0020 | -1.0020 | 1.1852 | 1.0011 | -1.0018 | 1.7029 |
| -1.150 | 1.0013 | -1.0000 | -0.2321 | 0.9994 | -1.0004 | 0.2121 | 0.9974 | -1.0012 | 0.6850 | 0.9953 | -1.0015 | 1.1816 | 0.9934 | -1.0007 | 1.6982 |
| -1.100 | 0.9982 | -0.9999 | -0.2327 | 0.9947 | -1.0001 | 0.2108 | 0.9920 | -1.0007 | 0.6829 | 0.9894 | -1.0005 | 1.1790 | 0.9870 | -0.9989 | 1.6952 |
| -1.050 | 0.9954 | -0.9997 | -0.2332 | 0.9916 | -0.9996 | 0.2101 | 0.9891 | -1.0001 | 0.6821 | 0.9870 | -0.9994 | 1.1787 | 0.9848 | -0.9970 | 1.6955 |
| -1.000 | 0.9941 | -0.9995 | -0.2332 | 0.9915 | -0.9992 | 0.2105 | 0.9903 | -0.9997 | 0.6831 | 0.9896 | -0.9986 | 1.1811 | 0.9886 | -0.9956 | 1.6997 |
| -0.950 | 0.9953 | -0.9993 | -0.2328 | 0.9950 | -0.9990 | 0.2120 | 0.9960 | -0.9997 | 0.6858 | 0.9972 | -0.9987 | 1.1856 | 0.9980 | -0.9957 | 1.7067 |
| -0.900 | 0.9986 | -0.9992 | -0.2319 | 1.0013 | -0.9990 | 0.2141 | 1.0044 | -1.0004 | 0.6891 | 1.0077 | -0.9999 | 1.1907 | 1.0104 | -0.9975 | 1.7142 |
| -0.850 | 1.0029 | -0.9992 | -0.2310 | 1.0080 | -0.9994 | 0.2160 | 1.0127 | -1.0017 | 0.6917 | 1.0172 | -1.0022 | 1.1942 | 1.0215 | -1.0009 | 1.7189 |
| -0.800 | 1.0065 | -0.9993 | -0.2303 | 1.0124 | -1.0001 | 0.2169 | 1.0171 | -1.0034 | 0.6921 | 1.0216 | -1.0050 | 1.1940 | 1.0265 | -1.0054 | 1.7182 |
| -0.750 | 1.0076 | -0.9994 | -0.2301 | 1.0121 | -1.0006 | 0.2162 | 1.0150 | -1.0049 | 0.6896 | 1.0178 | -1.0075 | 1.1892 | 1.0220 | -1.0095 | 1.7107 |
| -0.700 | 1.0051 | -0.9993 | -0.2306 | 1.0062 | -1.0008 | 0.2140 | 1.0055 | -1.0054 | 0.6846 | 1.0051 | -1.0083 | 1.1807 | 1.0071 | -1.0115 | 1.6978 |
| -0.650 | 0.9995 | -0.9990 | -0.2315 | 0.9962 | -1.0003 | 0.2111 | 0.9910 | -1.0044 | 0.6787 | 0.9866 | -1.0065 | 1.1713 | 0.9850 | -1.0095 | 1.6831 |
| -0.600 | 0.9925 | -0.9982 | -0.2323 | 0.9855 | -0.9990 | 0.2086 | 0.9766 | -1.0018 | 0.6744 | 0.9682 | -1.0017 | 1.1647 | 0.9624 | -1.0030 | 1.6723 |
| -0.550 | 0.9869 | -0.9971 | -0.2326 | 0.9792 | -0.9974 | 0.2080 | 0.9687 | -0.9983 | 0.6741 | 0.9581 | -0.9951 | 1.1649 | 0.9487 | -0.9935 | 1.6712 |
| -0.500 | 0.9852 | -0.9959 | -0.2316 | 0.9817 | -0.9963 | 0.2100 | 0.9735 | -0.9957 | 0.6791 | 0.9636 | -0.9895 | 1.1740 | 0.9533 | -0.9851 | 1.6831 |
| -0.450 | 0.9884 | -0.9944 | -0.2295 | 0.9948 | -0.9966 | 0.2143 | 0.9935 | -0.9959 | 0.6884 | 0.9887 | -0.9884 | 1.1907 | 0.9812 | -0.9829 | 1.7068 |
| -0.400 | 0.9944 | -0.9926 | -0.2263 | 1.0159 | -0.9990 | 0.2192 | 1.0259 | -1.0009 | 0.6987 | 1.0305 | -0.9949 | 1.2095 | 1.0298 | -0.9911 | 1.7349 |
| -0.375 | 0.9969 | -0.9914 | -0.2245 | 1.0272 | -1.0010 | 0.2210 | 1.0442 | -1.0055 | 0.7025 | 1.0545 | -1.0016 | 1.2170 | 1.0586 | -1.0001 | 1.7468 |
| -0.350 | 0.9979 | -0.9897 | -0.2226 | 1.0372 | -1.0035 | 0.2220 | 1.0615 | -1.0116 | 0.7044 | 1.0780 | -1.0107 | 1.2215 | 1.0876 | -1.0127 | 1.7549 |
| -0.325 | 0.9961 | -0.9874 | -0.2207 | 1.0442 | -1.0061 | 0.2217 | 1.0757 | -1.0188 | 0.7037 | 1.0986 | -1.0222 | 1.2218 | 1.1142 | -1.0289 | 1.7573 |
| -0.300 | 0.9904 | -0.9841 | -0.2187 | 1.0463 | -1.0085 | 0.2200 | 1.0846 | -1.0269 | 0.6996 | 1.1136 | -1.0358 | 1.2168 | 1.1353 | -1.0485 | 1.7523 |
| -0.275 | 0.9796 | -0.9794 | -0.2165 | 1.0418 | -1.0102 | 0.2168 | 1.0857 | -1.0351 | 0.6919 | 1.1202 | -1.0507 | 1.2055 | 1.1477 | -1.0708 | 1.7384 |
| -0.250 | 0.9626 | -0.9728 | -0.2138 | 1.0289 | -1.0103 | 0.2123 | 1.0769 | -1.0425 | 0.6805 | 1.1155 | -1.0658 | 1.1878 | 1.1479 | -1.0944 | 1.7150 |
| -0.225 | 0.9386 | -0.9637 | -0.2103 | 1.0063 | -1.0080 | 0.2068 | 1.0562 | -1.0479 | 0.6657 | 1.0971 | -1.0794 | 1.1638 | 1.1328 | -1.1172 | 1.6819 |
| -0.200 | 0.9070 | -0.9512 | -0.2054 | 0.9731 | -1.0021 | 0.2012 | 1.0222 | -1.0493 | 0.6486 | 1.0632 | -1.0890 | 1.1346 | 1.0999 | -1.1360 | 1.6402 |
| -0.175 | 0.8677 | -0.9346 | -0.1985 | 0.9290 | -0.9909 | 0.1965 | 0.9746 | -1.0447 | 0.6305 | 1.0127 | -1.0916 | 1.1021 | 1.0478 | -1.1470 | 1.5921 |
| -0.150 | 0.8209 | -0.9129 | -0.1887 | 0.8742 | -0.9728 | 0.1941 | 0.9136 | -1.0315 | 0.6136 | 0.9461 | -1.0836 | 1.0689 | 0.9767 | -1.1452 | 1.5410 |
| -0.125 | 0.7674 | -0.8850 | -0.1750 | 0.8101 | -0.9459 | 0.1959 | 0.8407 | -1.0066 | 0.6005 | 0.8652 | -1.0609 | 1.0387 | 0.8887 | -1.1253 | 1.4915 |
| -0.100 | 0.7084 | -0.8497 | -0.1561 | 0.7383 | -0.9081 | 0.2039 | 0.7584 | -0.9668 | 0.5946 | 0.7731 | -1.0190 | 1.0159 | 0.7875 | -1.0813 | 1.4494 |
| -0.075 | 0.6455 | -0.8060 | -0.1309 | 0.6614 | -0.8573 | 0.2205 | 0.6700 | -0.9092 | 0.5988 | 0.6742 | -0.9532 | 1.0057 | 0.6785 | -1.0072 | 1.4212 |
| -0.050 | 0.5805 | -0.7528 | -0.0983 | 0.5821 | -0.7913 | 0.2482 | 0.5791 | -0.8307 | 0.6172 | 0.5731 | -0.8600 | 1.0126 | 0.5676 | -0.8972 | 1.4140 |
| -0.025 | 0.5154 | -0.6872 | -0.0550 | 0.5035 | -0.7081 | 0.2896 | 0.4898 | -0.7250 | 0.6568 | 0.4748 | -0.7330 | 1.0444 | 0.4608 | -0.7463 | 1.4353 |
| 0.000 | 0.4521 | -0.6119 | -0.0032 | 0.4283 | -0.6061 | 0.3472 | 0.4056 | -0.5967 | 0.7145 | 0.3836 | -0.5725 | 1.1030 | 0.3632 | -0.5507 | 1.4916 |
| 0.025 | 0.3923 | -0.5347 | 0.0495 | 0.3589 | -0.5000 | 0.4070 | 0.3296 | -0.4615 | 0.7762 | 0.3029 | -0.4016 | 1.1678 | 0.2785 | -0.3406 | 1.5568 |
| 0.050 | 0.3373 | -0.4635 | 0.0959 | 0.2969 | -0.4048 | 0.4553 | 0.2634 | -0.3354 | 0.8278 | 0.2345 | -0.2439 | 1.2180 | 0.2085 | -0.1466 | 1.6039 |
| 0.075 | 0.2877 | -0.4011 | 0.1334 | 0.2428 | -0.3194 | 0.4937 | 0.2075 | -0.2239 | 0.8648 | 0.1783 | -0.1013 | 1.2537 | 0.1527 | 0.0324 | 1.6371 |
| 0.100 | 0.2437 | -0.3450 | 0.1647 | 0.1967 | -0.2425 | 0.5241 | 0.1614 | -0.1223 | 0.8932 | 0.1335 | 0.0299 | 1.2803 | 0.1096 | 0.1979 | 1.6603 |
| 0.125 | 0.2053 | -0.2944 | 0.1910 | 0.1579 | -0.1732 | 0.5481 | 0.1241 | -0.0294 | 0.9148 | 0.0986 | 0.1501 | 1.2993 | 0.0773 | 0.3510 | 1.6763 |
| 0.150 | 0.1721 | -0.2491 | 0.2126 | 0.1258 | -0.1103 | 0.5669 | 0.0945 | 0.0553 | 0.9308 | 0.0720 | 0.2606 | 1.3130 | 0.0537 | 0.4923 | 1.6871 |
| 0.200 | 0.1194 | -0.1712 | 0.2453 | 0.0784 | -0.0009 | 0.5930 | 0.0533 | 0.2047 | 0.9514 | 0.0373 | 0.4556 | 1.3296 | 0.0248 | 0.7421 | 1.6993 |
| 0.250 | 0.0819 | -0.1073 | 0.2674 | 0.0478 | 0.0908 | 0.6086 | 0.0292 | 0.3316 | 0.9625 | 0.0187 | 0.6207 | 1.3377 | 0.0110 | 0.9504 | 1.7046 |
| 0.300 | 0.0556 | -0.0540 | 0.2822 | 0.0286 | 0.1687 | 0.6179 | 0.0156 | 0.4400 | 0.9683 | 0.0091 | 0.7603 | 1.3416 | 0.0047 | 1.1205 | 1.7069 |
| 0.350 | 0.0375 | -0.0092 | 0.2922 | 0.0169 | 0.2354 | 0.6233 | 0.0082 | 0.5327 | 0.9712 | 0.0043 | 0.8775 | 1.3434 | 0.0020 | 1.2566 | 1.7079 |
| 0.400 | 0.0251 | 0.0291 | 0.2988 | 0.0099 | 0.2928 | 0.6265 | 0.0042 | 0.6119 | 0.9728 | 0.0020 | 0.9748 | 1.3442 | 0.0008 | 1.3640 | 1.7083 |
| 0.450 | 0.0168 | 0.0620 | 0.3033 | 0.0058 | 0.3423 | 0.6283 | 0.0021 | 0.6791 | 0.9735 | 0.0009 | 1.0543 | 1.3446 | 0.0003 | 1.4477 | 1.7084 |
| 0.500 | 0.0112 | 0.0907 | 0.3062 | 0.0033 | 0.3850 | 0.6293 | 0.0010 | 0.7359 | 0.9739 | 0.0004 | 1.1183 | 1.3448 | 0.0001 | 1.5123 | 1.7085 |
| 0.550 | 0.0074 | 0.1158 | 0.3082 | 0.0019 | 0.4219 | 0.6299 | 0.0005 | 0.7835 | 0.9740 | 0.0002 | 1.1692 | 1.3449 | 0.0001 | 1.5617 | 1.7085 |
| 0.600 | 0.0049 | 0.1379 | 0.3095 | 0.0011 | 0.4538 | 0.6303 | 0.0002 | 0.8231 | 0.9741 | 0.0001 | 1.2093 | 1.3449 | 0.0000 | 1.5990 | 1.7085 |
| 0.650 | 0.0033 | 0.1574 | 0.3103 | 0.0006 | 0.4813 | 0.6305 | 0.0001 | 0.8551 | 0.9742 | 0.0000 | 1.2405 | 1.3449 | 0.0000 | 1.6271 | 1.7085 |
| 0.700 | 0.0022 | 0.1747 | 0.3109 | 0.0004 | 0.5049 | 0.6306 | 0.0001 | 0.8804 | 0.9742 | 0.0000 | 1.2648 | 1.3449 | 0.0000 | 1.6481 | 1.7085 |
| 0.750 | 0.0014 | 0.1902 | 0.3113 | 0.0002 | 0.5251 | 0.6306 | 0.0000 | 0.9003 | 0.9742 | 0.0000 | 1.2835 | 1.3449 | 0.0000 | 1.6638 | 1.7085 |
| 0.800 | 0.0010 | 0.2039 | 0.3115 | 0.0001 | 0.5422 | 0.6307 | 0.0000 | 0.9159 | 0.9742 | 0.0000 | 1.2979 | 1.3449 | 0.0000 | 1.6754 | 1.7085 |
| 0.850 | 0.0006 | 0.2162 | 0.3117 | 0.0001 | 0.5568 | 0.6307 | 0.0000 | 0.9281 | 0.9742 | 0.0000 | 1.3090 | 1.3449 | 0.0000 | 1.6840 | 1.7085 |
| 0.900 | 0.0004 | 0.2271 | 0.3118 | 0.0000 | 0.5691 | 0.6307 | 0.0000 | 0.9378 | 0.9742 | 0.0000 | 1.3174 | 1.3449 | 0.0000 | 1.6904 | 1.7085 |
| 0.950 | 0.0003 | 0.2369 | 0.3119 | 0.0000 | 0.5794 | 0.6307 | 0.0000 | 0.9454 | 0.9742 | 0.0000 | 1.3239 | 1.3449 | 0.0000 | 1.6951 | 1.7085 |
| 1.000 | 0.0002 | 0.2457 | 0.3119 | 0.0000 | 0.5880 | 0.6307 | 0.0000 | 0.9513 | 0.9742 | 0.0000 | 1.3289 | 1.3449 | 0.0000 | 1.6986 | 1.7085 |

$v_{xc}$ which vanishes exponentially as $x\to\infty$, whereas one would expect that the correct $v_{xc}$ would behave like the classical image potential,[21] i.e.,

$$v_{\rm image}=-1/4x\,. \tag{2.17}$$

To assess the quantitative importance of this failure of our approximation, we have carried out the following control calculations. Up to the point $x_o$ where $v_{\rm eff}=0$, we used the form previously employed for $v_{\rm eff}$. However, for $x>x_o$, $v_{\rm eff}$ was taken to have the image form $\Phi-1/4x$, with $\Phi$ computed from (2.16c) and (2.7). The problem was then solved, for $r_s=2.5$ and 5, requiring self-consistency of $n(x)$. Fortunately, the densities in these calculations were found to differ from those previously obtained by no more than 1.2% of $\bar{n}$ for $r_s=5$, and no more than 0.3% for $r_s=2.5$. It thus appears that our use of the form (2.16b) for $v_{\rm eff}$

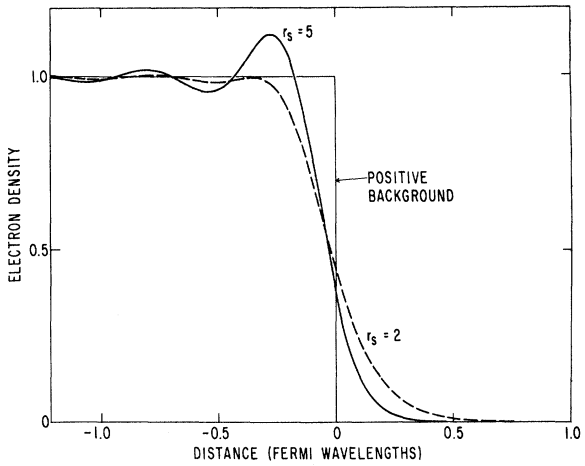


FIG. 2. Self-consistent charge density near metal surface for $r_s = 2$ and $r_s = 5$ (uniform positive background model).

also in the region outside of the metal surface, where it is not correct, does not introduce serious errors into the density distributions. In addition, we shall see in Sec. II C that the correlation contribution to the surface energy is a relatively small fraction of the experimental value, and thus, in discussing surface energies, errors due to an inadequate treatment of correlation effects should not be important.

### C. Surface Energies

The surface energy $\sigma$ of a crystal is the energy required, per unit area of new surface formed, to split the crystal in two along a plane. The total energy of the crystal, split or unsplit, can be written as a sum of three terms

$$E = T_s[n] + E_{xc}[n] + E_{es}[n] \ . \qquad (2.18)$$

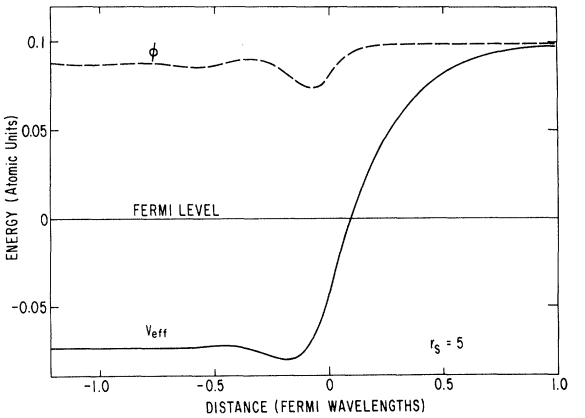


FIG. 3. Effective one-electron potential $v_{eff}$, with electrostatic part $\varphi$, near metal surface (positive background model; $r_s = 5$).

Here the first two terms represent, as before, kinetic, exchange, and correlation contributions to the electronic energy [see Eq. (2.2)]. The last term $E_{es}$ is the total classical electrostatic energy of all positive and negative charge densities:

$$E_{es} = \frac{1}{2}\int \frac{(n(\vec{r}) - n_+(\vec{r}))\,(n(\vec{r}\,') - n_+(\vec{r}\,'))}{|\vec{r} - \vec{r}\,'|}\, d\vec{r}\, d\vec{r}\,'$$

$$= \tfrac{1}{2}\int \varphi[n; \vec{r}\,]\,(n(\vec{r}) - n_+(\vec{r}))\, d\vec{r} \ , \qquad (2.19)$$

where $\varphi$, the total electrostatic potential energy of an electron, is given by[22]

$$\varphi[n; \vec{r}\,] = \int \frac{(n(\vec{r}\,') - n_+(\vec{r}\,'))}{|\vec{r} - \vec{r}\,'|}\, d\vec{r}\,' \ . \qquad (2.20)$$

Corresponding to (2.18), the surface energy of the uniform background model may be written as a sum of three terms

$$\sigma_u = \sigma_s + \sigma_{xc} + \sigma_{es} \ . \qquad (2.21)$$

For $\sigma_s$ we can take over the analysis presented by Huntington,[23] which gives

$$\sigma_s = \frac{1}{2\pi^2}\int_0^{k_F} \left(\frac{\pi}{4} - \gamma(k)\right)(k_F^2 - k^2)\, k\, dk$$

$$- \int_{-\infty}^{\infty} \{v_{eff}[n; x] - v_{eff}[n; -\infty]\}\, n(x)\, dx \ . \qquad (2.22)$$

The other two terms are, in the present model,

$$\sigma_{xc} = \int_{-\infty}^{\infty} [\epsilon_{xc}(n(x)) - \epsilon_{xc}(\bar{n})]\, n(x)\, dx \qquad (2.23)$$

and $$\sigma_{es} = \tfrac{1}{2}\int_{-\infty}^{\infty} \varphi[n; x]\,(n(x) - n_+(x))\, dx \ . \qquad (2.24)$$

Table II lists the magnitudes of $\sigma_u$ and its three components for different values of $r_s$. First, we observe that the kinetic-energy contribution $\sigma_s$ is negative, reflecting the fact that in the split crystal, the electron density is more spread out. Second, we note that over the entire density range $\sigma_{xc} \gg \sigma_{es}$, showing that Thomas-Fermi or Hartree calculations are completely useless for quantita-

TABLE II. The surface energy $\sigma_u$ and its components in the uniform background model. $\sigma_{xc} \equiv \sigma_x + \sigma_c$; $\sigma_u = \sigma_s + \sigma_{xc} + \sigma_{es}$. Units are ergs/cm$^2$.

| $r_s$ | $\sigma_s$ | $\sigma_x$ | $\sigma_c$ | $\sigma_{es}$ | $\sigma_u$ |
|---|---|---|---|---|---|
| 2.0 | −5600 | 3080 | 180 | 1330 | −1010 |
| 2.5 | −1850 | 1350 | 110 | 430 | 40 |
| 3.0 | − 720 | 680 | 70 | 170 | 200 |
| 3.5 | − 320 | 380 | 50 | 80 | 190 |
| 4.0 | − 145 | 230 | 35 | 40 | 160 |
| 4.5 | − 70 | 140 | 25 | 25 | 120 |
| 5.0 | − 30 | 95 | 20 | 15 | 100 |
| 5.5 | − 15 | 65 | 15 | 10 | 75 |
| 6.0 | − 5 | 45 | 10 | 10 | 60 |

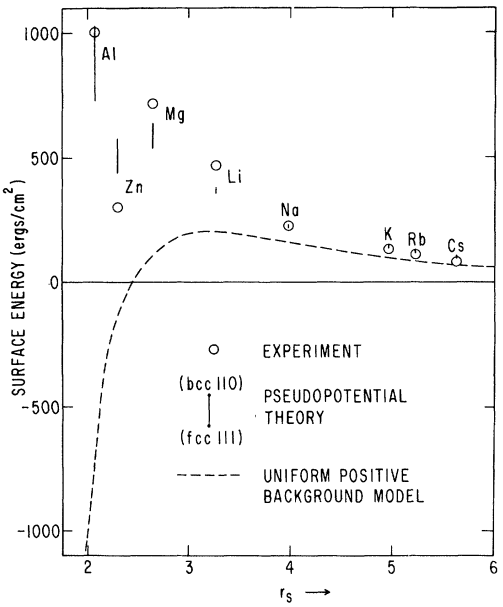


FIG. 4. Comparison of theoretical values of the surface energy with zero-temperature extrapolations of experimental results for liquid-metal surface tensions (open circles). Dashed curve gives the surface energy for the positive background model. Vertical lines give theoretical values corrected for the presence of the lattice: The lower end point gives the value appropriate to an fcc lattice, the upper end point that appropriate to a bcc lattice. In both cases, the surface plane is taken to be that lattice plane which is most densely packed. For the alkali metals of lower density, the lines are contracted almost to points.

tive purposes. Finally, we note that, particularly at higher densities, there are large cancellations between positive and negative terms, making the final results rather sensitive to small errors in the individual terms. Over the range $r_s = 3$–$5$, covering the alkali metals Li, Na, K, for which Smith[10] gives calculated surface energies, our results exceed his by about 50%.

In Fig. 4, the calculated surface energies are compared with linear extrapolations to zero temperature of measured liquid-metal surface tensions.[24] The agreement between theory and experiment is fair for the lower-density alkali metals, but for higher-density metals the measured surface tensions increase rapidly with density, while the calculated surface energies decrease towards large negative values. This basic shortcoming of the uniform background model, which all previous calculations have also encountered, will be corrected in the following section by going over to a model in which the positive ions are more realistically treated. The correlation contribution to the calculated $\sigma$ (Table II) is never more than about 15% of the experimental value, indicating that errors in $\sigma$ introduced by the approximate treatment of correlations are not significant.

## III. ION LATTICE MODEL

### A. Theory

In the present section, we shall calculate the surface energy on the basis of a model in which the ions, situated on the sites of a regular half-lattice,[25] are represented by appropriate pseudopotentials. Such a model is known to be quantitatively successful for simple bulk metals in which the conduction band has $s$-$p$ character and is adequately separated from $d$-like states.

For these metals, the difference between the total pseudopotential and the potential due to the uniform charge background is small.[26] Therefore, taking advantage of the stationary property[7] of expression (2.2) for $E_v[n]$, we shall calculate all energies in the present model using the electronic density distributions $n(x)$ of the uniform background model. In this way, we avoid the much more difficult problem of solving truly 3-dimensional Schrödinger equations.

We adopt here the local ion pseudopotential proposed by Ashcroft,[27] which has the form

$$v_{ps}(\vec{r}) = 0, \quad r \le r_c$$
$$= -\frac{Z}{r}, \quad r > r_c \tag{3.1}$$

where $Z$ is the ionic charge and $r_c$ is a cutoff radius which has been determined for each metal to give a good description of the bulk properties. This is equivalent to representing each ion by an effective charge distribution $n_{ion}(\vec{r})$ which gives rise to the potential (3.1).

Since in the present model, the electron densities $n(x)$ of the uniform background case are employed, the intrinsic electronic energies $T_s[n]$ and $E_{xc}[n]$ are the same as before. The difference of the surface energies in the two models,

$$\delta\sigma = \sigma - \sigma_u \ , \tag{3.2}$$

is therefore entirely due to the differences in electrostatic interaction energies of all positive and

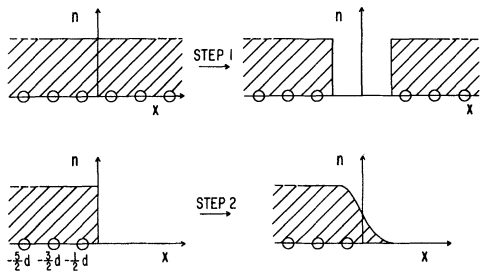


FIG. 5. Two steps for calculating the electrostatic contributions to the surface energy $\sigma$.

TABLE III. Cleavage energy constants $\alpha$.[a]

| Lattice type | Cleavage planes (111) | (100) | (110) |
|---|---|---|---|
| fcc | 0.003 25 | 0.014 34 | 0.044 07 |
| bcc | 0.032 06 | 0.031 00 | 0.005 63 |

[a]We would like to thank M. Rao for his help with the computations of $\alpha$.

negative charges [including the effective ionic charges $n_{\text{ion}}(\vec{r})$].

We recall the definition of surface energy as the energy required, per unit area of new surface formed, to split the crystal in two. For each of the two models, we calculate the electrostatic contribution to the surface energy in two steps (see Fig. 5):

*Step* 1. We divide the crystal in two, holding the electron density uniform up to the nominal metal boundary in each half. The contribution to $\delta\sigma$ from this step is a classical cleavage energy which will be denoted by $\delta\sigma_{\text{cl}}$.

*Step* 2. Next we change, in both models, the electron density from its step-function form to its actual form $n(x)$. The contribution from this step to $\delta\sigma$ will be called $\delta\sigma_{\text{ps}}$.

Step 1 requires no energy in the uniform background model. In the ion lattice model we may, in calculating the energy required for this step, replace the pseudopotentials by point-charge potentials.[28] A dimensional argument shows that, for a given lattice type and a given cleavage plane

$$\delta\sigma_{\text{cl}} = \alpha Z \bar{n} , \tag{3.3}$$

where $\alpha$ is a dimensionless constant. The computation of this constant is described in Appendix C. The results for the body-centered and face-centered cubic lattices with cleavage planes perpendicular to the [100], [111], and [110] directions are given in Table III.

Step 2, as inspection of Fig. 5 shows, contributes the following term to $\delta\sigma$:

$$\delta\sigma_{\text{ps}} = \int_{-\infty}^{\infty} \delta v(x)[n(x) - n_+(x)]\, dx . \tag{3.4}$$

Here $\delta v(x)$ is the average, over the $y$-$z$ plane, of the sum of the ionic pseudopotentials of the half-lattice, minus the potential due to the semi-infinite uniform charge background. The algebraic expression for $\delta v(x)$ is derived in Appendix D. The two factors entering the integrand in (3.4) are plotted in Fig. 6.

The total surface energy in the present model is then given by

$$\sigma = \sigma_u + \delta\sigma_{\text{cl}} + \delta\sigma_{\text{ps}} , \tag{3.5}$$

where $\sigma_u$ is the surface energy in the uniform background model and $\delta\sigma_{\text{cl}}$ and $\delta\sigma_{\text{ps}}$ are given by Eqs. (3.3) and (3.4).

### B. Computations and Comparison with Experiment

Since there are practically no data available for the surface energies of simple metals in the solid phase, we have computed values of $\sigma$ which would be most appropriate for comparison with measurements of the surface tensions of liquid metals. In the absence of a satisfactory theory for the ionic configurations of liquid-metal surfaces, we have calculated $\sigma$ for such ordered lattice structures and cleavage planes as, in our view, resembled most closely a liquid surface. Experimental evidence for local order in the liquid state, similar to that in the solid state, provides some justification for this approach.[29]

The coordination numbers, in the liquid state, of the metals considered lie between the coordination numbers of the bcc and fcc lattices, which are 8 and 12, respectively.[29] Therefore, calculations were carried out for both of these two lattice types. The faces selected were those most densely packed, (111) for fcc and (110) for bcc. Such a choice has been considered reasonably representative of a liquid surface by various authors,[30] and we have verified by sample calculations that it was indeed these faces which had the lowest energies and hence would be expected to appear on the surface.

We have calculated surface energies for the 8 metals listed in Table IV. These include all of those considered in the bulk pseudopotential calcu-

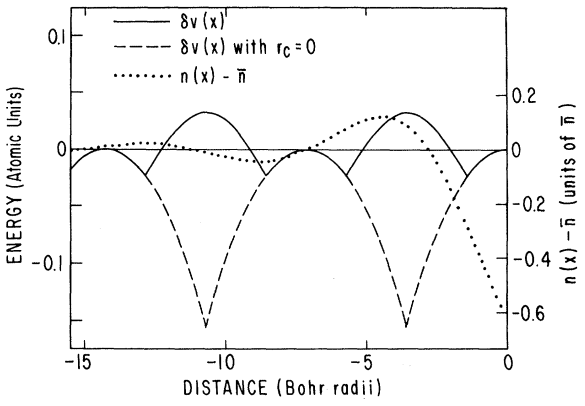


FIG. 6. Factors in the integrand giving $\delta\sigma_{\text{ps}}$ [Eq. (3.4)]. The case of potassium is shown here. In the absence of pseudopotential cancellation, $\delta v(x)$ is the function represented by the deeply cusped dashed line (the lattice planes are at the cusps). The presence of substantial oscillations in $n(x) - n_+(x)$ has in general an important effect on the value of $\delta\sigma_{\text{ps}}$.

TABLE IV. Surface energies in the ion lattice model for eight simple metals. The table gives total surface energy $\sigma$ and its component parts ($\sigma = \sigma_u + \delta\sigma_{ps} + \delta\sigma_{cl}$) for the lattice structures and surface planes indicated. Units are ergs/cm$^2$. Also included are $r_s$ values, and values for the pseudopotential radius $r_c$ (Ref. 3).

| Metal | $r_s$ | $r_c$ | $\sigma_u$ | $\delta\sigma_{ps}$ | $\delta\sigma_{cl}$ | | $\sigma$[a] | |
|---|---|---|---|---|---|---|---|---|
| | | | | | fcc(111) | bcc(110) | fcc(111) | bcc(110) |
| Al | 2.07 | 1.12 | −730 | 1050 | 408 | 708 | 730 | 1030 |
| Zn | 2.30 | 1.27 | −130 | 370 | 197 | 342 | 440 | 580 |
| Mg | 2.65 | 1.39 | 110 | 300 | 130 | 226 | 540 | 640 |
| Li | 3.28 | 1.06 | 210 | 110 | 35 | 61 | 360 | 380 |
| Na | 3.99 | 1.67 | 160 | 35 | 19 | 33 | 210 | 230 |
| K | 4.96 | 2.14 | 100 | 25 | 10 | 17 | 140 | 140 |
| Rb | 5.23 | 2.61 | 85 | 20 | 8 | 15 | 110 | 120 |
| Cs | 5.63 | 2.93 | 70 | 20 | 7 | 12 | 100 | 100 |

[a]Rounded values.

lations of Ashcroft and Langreth,[3] with the exception of Pb to which we shall return later. The calculations were carried out for mean densities $\bar{n}$ appropriate to the solid, using the values for the pseudopotential radius $r_c$, given in Ref. 3.

Since for given $\bar{n}$, the lattice-plane spacings of the densest bcc and fcc faces are within 3% of one another, a difference which has been neglected, $\delta\sigma_{ps}$, shown in column 5 of Table IV, is the same for the two types of faces. On the other hand, the classical cleavage energies, $\delta\sigma_{cl}$, shown in columns 6 – 9, differ rather considerably. This difference is reflected in the total surface energies $\sigma$ listed in columns 8 and 9.

We note that both $\delta\sigma_{ps}$ and $\delta\sigma_{cl}$ are positive and become quite large for the higher-density metals. Together they more than compensate for the negative values of $\sigma_u$.

Our final results are plotted in Fig. 4, where they are denoted "pseudopotential theory." The results for fcc (111) and bcc (110) faces are joined by vertical lines. These lines may be regarded as a rough measure of the uncertainties introduced into our estimates for liquid-metal surface tensions by our present very incomplete knowledge of the ionic configurations near a liquid surface. The same figure shows also the results of the uniform model and experimentally measured surface tensions.[31] It should be mentioned that particularly for Zn, there are still considerable discrepancies among the data obtained by different workers.[32]

We note that passing from the uniform to the ion lattice model leads to relatively small changes for the low-density alkali metals Cs, Rb, and K, with an indication of slightly improved agreement with experiment. On the other hand for the denser metals Na, Li, Mg, Zn, and Al, the differences between the two models become progressively greater, and while the uniform model eventually fails completely, the ion lattice model follows the experimental trends quite well, a typical error for these metals being about 25%.[33]

We omitted the case of Pb from the above considerations. For this metal the measured surface tension extrapolates to 620 ergs/cm$^2$ at zero temperature,[34] while our calculations gave a mean value of of 1400 ergs/cm$^2$. We have no real explanation of this large discrepancy at this time. It may be noted, however, that Ashcroft and Langreth,[3] in their pseudopotential calculations of bulk energies, also found rather less satisfactory agreement for Pb than for the other metals. We also remark that, unlike the other metals considered, Pb is tetravalent, and that furthermore, it has by far the highest atomic number.

In all the above described calculations the ion half-lattice was undistorted. In Appendix E, we show that allowing the surface plane of ions to relax to a position of lower energy has a negligible effect on the calculated surface energies.

## IV. CONCLUDING REMARKS

This paper reports the results of calculations of the electron density distributions and surface energies of simple metals. Many-body effects are taken approximately into account by the use of local effective exchange and correlation energies [Eq. (2.14)]. The interactions of electrons and ions are represented by pseudopotentials taken from theories of bulk metals. All electrostatic energies, including an important classical cleavage energy, are included.

The results are compared with experimental data on surface tensions of eight liquid metals, Li, Na, K, Rb, Cs, Mg, Zn, and Al, whose surface electron densities vary by a factor of 20 and whose surface energies range from 80 to 1000 ergs/cm$^2$. For this entire set of metals, we find good semiquantitative agreement, typical errors being about 25%. In the case of the lower-density alkalis the agreement is especially close. For a ninth metal, Pb, the theoretical surface energy is too high by a factor of about 2.

In spite of the unexplained failure for Pb, we believe that we have come a substantial step closer to a quantitative theory of the electronic structure of metal surfaces.

Effects which we have presumed to be small but which need to be further examined include second-order pseudopotential terms and contributions to the surface energy from changes of the zero point lattice vibrations.[35]

More fundamental remaining questions concern the use of local exchange and correlation energies; the use of pseudopotentials, designed for bulk metals, in the surface region; and the simulation of a liquid-metal surface by an appropriate face of a solid metal.

It is hoped that additional good experimental data for both liquid and solid metals will become available to allow a wider test of the theory and perhaps to suggest necessary modifications.


## ACKNOWLEDGMENTS

We would like to thank J. Rudnick for helpful discussions. The assistance of the staff of the UCSD Computation Center is also very much appreciated.


## APPENDIX A: FRIEDEL OSCILLATIONS

### 1. General Forms: Importance in Numerical Calculations

Substitution of the sine-wave form of $\psi_k(x)$ into Eq. (2.16d) yields the well-known result

$$n(x) \underset{x\to-\infty}{\sim} \bar{n}\left[1+\frac{3\zeta\cos 2(k_F x-\gamma_F)}{(2k_F x)^2}+O\left(\frac{1}{x^3}\right)\right], \quad \text{(A1)}$$

where $\zeta=1$ and $\gamma_F \equiv \gamma(k_F)$. Use of this form for $n(x)$ in Eq. (2.16b) then gives

$$v_{\text{eff}}[n;x] \underset{x\to-\infty}{\sim} -\tfrac{1}{2}k_F^2 + \mu_c'(\bar{n})\frac{3\zeta\bar{n}\cos 2(k_F x-\gamma_F)}{(2k_F x)^2}+O\left(\frac{1}{x^3}\right), \quad \text{(A2)}$$

with $\mu_c'(n)$ the derivative with respect to density of the correlation part of $\mu_{xc}(n)$. The oscillatory terms in the electrostatic and exchange potentials, it is found, cancel each other exactly in the asymptotic region. The solution $\psi_k(x)$ of Eq. (2.16a) for the potential of Eq. (A2), in turn, also exhibits a correction of $O(x^{-2})$:

$$\psi_k(x) \underset{x\to-\infty}{\sim} \sin[kx-\gamma(k)] - \frac{\zeta\mu_c'(\bar{n})}{16\pi^2x^2}\left\{\frac{\sin[(k+2k_F)x-\gamma(k)-2\gamma_F]}{k+k_F} - \frac{\sin[(k-2k_F)x-\gamma(k)+2\gamma_F]}{k-k_F}\right\}+O\left(\frac{1}{x^3}\right). \quad \text{(A3)}$$

Taking proper account of these $O(x^{-2})$ corrections was found to be important in the actual calculation. The computations implied by Eqs. (2.16) are carried into the metal to a point $x_{\min}$, at which $\Phi$ and the wave-function renormalization constant are presumably chosen so that $v_{\text{eff}}[n; x_{\min}] = -\frac{1}{2}k_F^2$ and $\psi_k(x)$ matches a pure sine wave of unit amplitude. In order that these choices represent an adequate approximation to the $x_{\min}\to-\infty$ limit, however, the $O(x^{-2})$ terms must first be separated out from the computed values of $v_{\text{eff}}[n;x]$ and $\psi_k(x)$. Making $|x_{\min}|$ so large that these terms become unimportant leads to numerical instabilities.

### 2. Amplitude

The condition that the Friedel oscillations in $n(x)$ be self-consistent in the asymptotic region leads to the requirement that the $\zeta$ of Eq. (A1) be given by the relation

$$\zeta = [1+k_F\,\mu_c'(\bar{n})/(2\pi^2)]^{-1}.$$

This result is obtained by substituting the form given for $\psi_k(x)$ in Eq. (A3) into Eq. (2.16d). The parameter $\zeta$ is found to increase from 1.004 at $r_s=2$ to 1.07 at $r_s=6$ (using Wigner's formula[19] for $\epsilon_{xc}$ to obtain $\mu_c'$). The fact that the oscillations in the $r_s=2$ curve of Fig. 2 are so much smaller than those at $r_s=5$ is clearly not accounted for by this small variation in $\zeta$. The reason for the difference is rather as follows.

From Eq. (3.16) of Ref. 36, it is seen that quantum density oscillations of the type analyzed here are reduced in general by inverse powers of the integral

$$\tilde{x} \equiv k_F\int_x^{x_0} dt\{-2v_{\text{eff}}[n;t]\}^{-1/2}$$

(which tends toward $|x|$ as $x\to-\infty$). Here $x_0$ is the turning point ($v_{\text{eff}}[n;x_0]=\mu=0$). If $v_{\text{eff}}$ is taken to exhibit simple exponential decay toward $-\frac{1}{2}k_F^2$ to the left of $x_0$, with decay length $\lambda$, then $\tilde{x}\approx|x-x_F|^2$ for large $|x|$, with $x_F = 2\lambda\ln 2 + x_0$.

In the present calculation, $x_0$ (equal to 1.4 at $r_s=6$ and 2.4 at $r_s=2$) and the characteristic length $\lambda$ over which $v_{\text{eff}}$ varies, increase slowly as $r_s$ decreases. This means that in terms of the wavelength of the Friedel oscillations ($\pi/k_F$), $x_F$, the effective origin of $x$, rapidly moves further and further to the right as $r_s$ decreases. This implies, in turn, that the first oscillations to appear to the left of $x=0$ become smaller and smaller relative to $\bar{n}$ as $\bar{n}$ increases.

## APPENDIX B: SELF-CONSISTENCY PROCEDURE

The set of equations (2.16) in the order (c), (b), (a), (d) [with $n$ replaced by $n_1$ in (a), (b), (c) and by

$n_2$ in (d)] may be taken to define a functional $F$ that transforms one electron density into another:

$$n_2(x) = F[n_1; x] .$$

The self-consistent solution to Eqs. (2.16) is then $n(x) = F[n; x]$. The trial density $n_0(x)$ employed in finding this solution consisted of an exponential decaying toward $\bar{n}$ in a Thomas-Fermi length inside the metal, matched to a linear combination of two exponentials with adjustable decay lengths outside. A Gaussian (with its parameters adjustable) was added to simulate roughly the first large peak of the expected density oscillations, and the neutrality condition $\int_{-\infty}^{\infty}[n_0(x) - n_+(x)]\,dx = 0$ was imposed.

Straight iteration was found not to be a convergent solution procedure, and so an analog of the Newton-Raphson method, based on the use of the linear response function $\delta F/\delta n$, was employed. An $n_0(x)$ was chosen and $n_1(x) = F[n_0; x]$ evaluated. A neutralizing charge distribution was added to $n_1$ in the surface region, in order that $dv_{\text{eff}}[n_1; x]/dx|_{x=-\infty}$ vanish, since the fact that $n_0$ obeys the neutrality condition does not guarantee that $n_1$ will obey it also. The function $n_2(x) = F[n_1; x]$ was then computed.

The trial density $n_0$ was readjusted until $n_1$ and $n_2$ were close to one another, implying that each was near the true solution. $n_1$ was then corrected by the addition of a linear combination of functions $\sum_{l=1}^{M} a_l u_l(x)$ with the $a_l$ determined by the self-consistency condition

$$n_1(x) + \sum_{l=1}^{M} a_l u_l(x) = n_2(x) + \sum_{l=1}^{M} a_l \times \int_{-\infty}^{\infty} \frac{\delta F[n_1; x]}{\delta n_1(x')}\, u_l(x')\,dx' \equiv \tilde{n}(x) , \qquad \text{(B1)}$$

projected onto a set of $M$ orthogonal functions. The $u_l$ were taken to be the derivatives (so as to preserve charge neutrality) of the first $M$ harmonic oscillator functions, with width and center chosen so as to localize them in the surface region, and Eq. (B1) was projected onto the oscillator functions themselves. The integral $\int_{-\infty}^{\infty} (\delta F/\delta n_1) u_l(x')\,dx'$ was found by computation of the expression $\lambda^{-1}(F[n_1 + \lambda u_l; x] - n_2(x))$ with $\lambda u_l(x) \ll \bar{n}$. Evaluating $n(x) \equiv F[\tilde{n}; x]$ (which is the function actually given in Table I) provided a direct check on the self-consistency of $\tilde{n}$. The procedure described here could be used repeatedly, but it proved unnecessary to do so (with $M = 8$).

It will, of course, be recognized that the asymptotic phase and amplitude of the Friedel oscillations in $\tilde{n}(x)$ are not affected by the addition of functions localized in the surface region [the $u_l(x)$]. This is not important, however, because these properties of $\tilde{n}(x)$ are already close to those of the true self-consistent solution. The phase difference between the oscillations in $\tilde{n}(x)$ and $n(x)$ was in fact found never to be more than 5° (this reflects an accurate choice of trial density), and the oscillation amplitude for $\tilde{n}(x)$ [corresponding to $\zeta = 1$ in Appendix A, since these oscillations are identical to those in $n_1(x)$] is constrained for theoretical reasons to be quite close to the correct value [i.e., the self-consistent $\zeta$ is close to unity (see Appendix A)].

## APPENDIX C: EVALUATION OF THE TERM $\delta\sigma_{\text{cl}}$ IN THE SURFACE ENERGY

It is useful for the following discussion to introduce the abbreviation $E(S, S')$ to refer to the interaction energy of $S$ and $S'$ per unit area normal to the $x$-direction, where the symbols $S$ and $S'$ may be replaced by "±" (denoting a rigid, uniform, positive or negative background) or "lat" (denoting the lattice). $E(S, S)$ is a self-energy. The charge distributions $S$ and $S'$ will be taken to occupy the half-space $x < 0$, unless the subscript "inf" is affixed to $E$, to indicate that they fill all of space [(i.e., that they refer to the uncleaved crystal) cf. Fig. 5]. The classical cleavage energy $\delta\sigma_{\text{cl}}$ is then

$$\delta\sigma_{\text{cl}} = E(\text{lat}, \text{lat}) + E(-, \text{lat}) + E(-, -) - \tfrac{1}{2}[E_{\text{inf}}(\text{lat}, \text{lat}) + E_{\text{inf}}(-, \text{lat}) + E_{\text{inf}}(-, -)].$$

The electron distribution of step 1 in Fig. 5 is considered to interact with the lattice via a pure Coulomb potential, rather than via a pseudopotential. This distinction affects the value of $\delta\sigma_{\text{cl}}$ only in the case in which the cleavage plane passes through an ion core ($r_c > \frac{1}{2}d$), which does not occur in the present calculations.

Simple considerations of electrostatics lead to the result

$$\delta\sigma_{\text{cl}} = E(\text{lat}, \text{lat}) + \tfrac{1}{2} E(-, \text{lat}) - \tfrac{1}{2}[E_{\text{inf}}(\text{lat}, \text{lat}) + \tfrac{1}{2} E_{\text{inf}}(-, \text{lat})]. \qquad \text{(C1)}$$

In evaluating this expression it is convenient to let $\Delta\varphi_{\text{lat}}(\nu)$ represent the Coulomb potential at lattice site $\nu$ due to all the ions of the semi-infinite lattice, minus that due to the ions of the infinite (uncleaved) lattice. Here the semi-infinite lattice is taken to be in the left half-space ($x < 0$), as is site $\nu$, which implies that $\Delta\varphi_{\text{lat}}(\nu)$ is simply the negative of the Coulomb potential at $\nu$ due to a semi-infinite lattice in the *right* half-space. It is convenient in addition to introduce the symbol $\Delta\varphi_{-}(\nu)$ to represent the corresponding difference of potentials due to semi-infinite ($x < 0$) and infinite negative backgrounds. This difference is then

the negative of the potential at $\nu$ due to such a semi-infinite background in the right half-space.

With $\Delta\varphi(\nu) \equiv \Delta\varphi_{\rm lat}(\nu) + \Delta\varphi_{-}(\nu)$, Eq. (C1) implies that

$$\delta\sigma_{\rm cl} = -\tfrac{1}{2}ZL^{-2}\sum_{\nu[L]} \Delta\varphi(\nu) \quad (L \to \infty). \tag{C2}$$

The symbol $\sum_{\nu[L]}$ stands for a summation over all lattice sites $\nu$ of the semi-infinite ($x < 0$) lattice which are in a volume bounded by the planes $y = \pm\frac{1}{2}L$, $z = \pm\frac{1}{2}L$. The actual calculation of $\Delta\varphi(\nu)$ will employ a technique for computing lattice sums discussed by Misra[37] and by van der Hoff and Benson,[38] and will follow in outline the treatment of the Coulomb problem for the infinite lattice given by Coldwell-Horsfall and Maradudin.[39]

For simplicity of exposition, the analysis presented here will be confined to the case of a simple cubic lattice of lattice constant $a$, cleaved along the (100) plane. The lattice planes are numbered by integers $k$, increasing from left to right, with $k < 0$ designating planes in the left half-space and $k \geq 0$ designating those in the right half-space. Since all of the sites in a given lattice plane are equivalent, the label $\nu$ used above may be replaced by the index $k$.

The two contributions to $\Delta\varphi(k)$, for $k < 0$, may be written

$$\Delta\varphi_{\rm lat}(k) = \frac{Z}{a}\sum_{j=-k}^{\infty}\sum_{mn}\frac{\exp[-(j^2+m^2+n^2)\epsilon]}{(j^2+m^2+n^2)^{1/2}}, \tag{C3}$$

with $\sum_{mn}$ extending over all integers, and

$$\Delta\varphi_{-}(k) = -\frac{Z}{a}\int_{-\infty}^{\infty}dy\int_{-\infty}^{\infty}dz\int_{-k-1/2}^{\infty}dx \times\frac{\exp[x^2+y^2+z^2)\epsilon]}{(x^2+y^2+z^2)^{1/2}}. \tag{C4}$$

The exponential convergence factor, with $\epsilon \to 0$, is introduced for convenience in treating singular terms; $\epsilon$ will be dropped at any point in the analysis at which its omission does not give rise to a divergence.

The use of Euler's representation of the $\Gamma$ function,

$$\frac{1}{u^x} = \frac{1}{\Gamma(x)}\int_0^{\infty} t^{x-1}e^{-ut}\,dt,$$

permits writing these expressions in the form

$$\Delta\varphi_{\rm lat}(k) = \frac{Z}{a\sqrt{\pi}}\sum_{j=-k}^{\infty}\sum_{mn}\int_0^{\infty}t^{-1/2} \times\exp[-(j^2+m^2+n^2)(t+\epsilon)]\,dt, \tag{C5a}$$

$$\Delta\varphi_{-}(k) = -\frac{Z\sqrt{\pi}}{a}\int_{-k-1/2}^{\infty}dx\int_{\epsilon}^{\infty}dt \times(t-\epsilon)^{-1/2}t^{-1}e^{-x^2t}. \tag{C5b}$$

The integration range in Eq. (C5a) is then divided into two segments at $t = \gamma^2$, allowing $\Delta\varphi_{\rm lat}(k)$ to be written as

$$\Delta\varphi_{\rm lat}(k) = \Delta\varphi_{\rm lat}^{(1)}(k) + \Delta\varphi_{\rm lat}^{(2)}(k), \tag{C6}$$

with $$\Delta\varphi_{\rm lat}^{(1)}(k) = \frac{Z}{a\sqrt{\pi}}\sum_{j=-k}^{\infty}\sum_{mn}\int_0^{\gamma^2}t^{-1/2} \times\exp[-(j^2+m^2+n^2)(t+\epsilon)]\,dt \tag{C7a}$$

and $$\Delta\varphi_{\rm lat}^{(2)}(k) = \frac{Z}{a}\sum_{j=-k}^{\infty}\sum_{mn}F(j,\ m,\ n,\ \gamma), \tag{C7b}$$

where $$F(x,\ y,\ z,\ \gamma) = \operatorname{erfc}[\gamma(x^2+y^2+z^2)^{1/2}] \times(x^2+y^2+z^2)^{-1/2}.$$

The separation parameter $\gamma$ is chosen later to achieve equally rapid rates of convergence for all of the series involved in $\Delta\varphi(k)$. The special case

$$\sum_{n=-\infty}^{\infty}e^{-n^2t} = \left(\frac{\pi}{t}\right)^{1/2}\sum_{n=-\infty}^{\infty}e^{-n^2\pi^2/t}$$

of Jacobi's imaginary transformation[40] for $\theta$ functions may be employed to put Eq. (C7a) into the form

$$\Delta\varphi_{\rm lat}^{(1)}(k) = \frac{Z}{2a}\sum_{j=-k}^{\infty}{\sum_{mn}}'G(j,\ m,\ n,\ \gamma) + \frac{Z\sqrt{\pi}}{a}\sum_{j=-k}^{\infty}\int_{\epsilon}^{\gamma^2}(t-\epsilon)^{-1/2}t^{-1}e^{-j^2t}\,dt, \tag{C8}$$

where

$$G(x,\ y,\ z,\ \gamma) = (y^2+z^2)^{-1/2}\{\exp[2\pi x(y^2+z^2)^{1/2}] \times\operatorname{erfc}[\pi\gamma^{-1}(y^2+z^2)^{1/2}+\gamma x] + \exp[-2\pi x(y^2+z^2)^{1/2}] \times\operatorname{erfc}[\pi\gamma^{-1}(y^2+z^2)^{1/2}-\gamma x]\}$$

and where the prime on the summation sign signifies omission of the $m = n = 0$ term.

The Coulomb singularities (for $\epsilon \to 0$) in the first two terms of the sum

$$\Delta\varphi(k) = \Delta\varphi_{-}(k) + \Delta\varphi_{\rm lat}^{(1)}(k) + \Delta\varphi_{\rm lat}^{(2)}(k)$$

then cancel in the following way:

$$\Delta\varphi_{-}(k) + \frac{Z\sqrt{\pi}}{a}\sum_{j=-k}^{\infty}\int_{\epsilon}^{\gamma^2}(t-\epsilon)^{-1/2}t^{-1}e^{-j^2t}\,dt = \frac{Z}{a}\sum_{j=-k}^{\infty}\left\{H(j,\ \gamma) + \pi^{3/2}\epsilon^{-1/2}\left[\operatorname{erfc}(j\epsilon^{1/2}) - \int_{j-1/2}^{j+1/2}\operatorname{erfc}(t\epsilon^{1/2})\,dt\right]\right\} \to \frac{Z}{a}\sum_{j=-k}^{\infty}H(j,\ \gamma) \quad \text{as } \epsilon \to 0.$$

Here $H(x, \gamma) = 2\pi x \operatorname{erfc}(\gamma x) - 2\pi^{1/2}\gamma^{-1} e^{-(\gamma x)^2}$ .

Note that this cancellation simply reflects the fact that a plane of ions $j$ together with a slab of the negative charge distribution extending a distance $\frac{1}{2}a$ on either side of the plane is neutral.

It is then easily seen that

$$\delta\sigma_{c1} = -\tfrac{1}{2}Z\bar{n}\sum_{l=1}^{\infty} l\Big[\sum_{mn} F(l, m, n, \gamma) + \tfrac{1}{4}\sum_{mn}{}' G(l, m, n, \gamma) + H(l, \gamma)\Big].$$

The choice $\gamma^2 \approx \pi$ leads to equally rapid convergence for all terms. With $\delta\sigma_{c1} = \alpha Z\bar{n}$, numerical computation shows that $\alpha = -0.00395$ [(100) face of simple cubic lattice]. (Results for fcc and bcc lattices are positive.)

The same procedure is employed for other lattice types and other crystal faces. The somewhat more generalized case[38, 40]

$$\sum_{n=-\infty}^{\infty} e^{-(n+c)^2 t} = \left(\frac{\pi}{t}\right)^{1/2} \sum_{n=-\infty}^{\infty} e^{-n^2\pi^2/t} \cos 2\pi nc$$

of Jacobi's transformation must be employed in these treatments.

## APPENDIX D: ALGEBRAIC EXPRESSION FOR $\delta v(x)$

Let $v_{ps}^{(\nu)}(\vec{r})$ be the pseudopotential at position $\vec{r}$ due to the ion at lattice site $\nu$ (which is at position $\vec{r}_\nu$). Further, let $\varphi_+(x)$ be the potential at $x$ due to a semi-infinite uniform positive background filling the half-space $x < 0$. Then

$$\delta v(x) \equiv \Big\langle \sum_{\nu(x<0)} v_{ps}^{(\nu)}(\vec{r}) \Big\rangle - \varphi_+(x) \quad , \tag{D1}$$

where the angular brackets denote an average over $y$ and $z$ directions, and where $\sum_{\nu(x<0)}$ denotes a summation over all sites of the semi-infinite lattice in the $x<0$ half-space. It is convenient to write

$$\delta v(x) = \delta v_1(x) + \delta v_2(x) \quad , \tag{D2}$$

where

$$\delta v_1(x) = \Big\langle \sum_{\nu(x<0)} (-Z|\vec{r} - \vec{r}_\nu|^{-1}) \Big\rangle - \varphi_+(x) \tag{D3a}$$

and

$$\delta v_2(x) = \sum_{\nu(x<0)} \langle v_{ps}^{(\nu)}(\vec{r}) + Z|\vec{r} - \vec{r}_\nu|^{-1} \rangle \quad . \tag{D3b}$$

The indicated average over $y$ and $z$ directions in Eq. (D3a) means that the charges at positions $\vec{r}_\nu$ can be regarded as smeared out uniformly over each lattice plane. The evaluation of $\delta v_1(x)$ is then a simple one-dimensional electrostatic problem, whose result is shown as a dashed line in Fig. 6. For $-d \le x \le 0$ (cf. Fig. 5),

$$\delta v_1(x) = -2\pi\bar{n}[x + d\theta(-x - \tfrac{1}{2}d)]^2 \, . \tag{D4}$$

Use of Ashcroft's form for the pseudopotential [Eq. (3.1)] implies that

$$v_{ps}^{(\nu)}(\vec{r}) + Z|\vec{r} - \vec{r}_\nu|^{-1} = Z|\vec{r} - \vec{r}_\nu|^{-1}\theta(r_c - |\vec{r} - \vec{r}_\nu|) \, . \tag{D5}$$

With the standard assumption of pseudopotential theory that the cores (the spherical regions of radius $r_c$ about each ion) are nonoverlapping, and under the condition $\frac{1}{2}d > r_c$, $\delta v_2(x)$ is easily seen to be a periodic function also, that tends to cancel $\delta v_1(x)$. For $-d \le x \le 0$,

$$\delta v_2(x) = 2\pi d\bar{n}(r_c - |x + \tfrac{1}{2}d|)\theta(r_c - |x + \tfrac{1}{2}d|) \, . \tag{D6}$$

## APPENDIX E: EQUILIBRIUM POSITION OF THE FIRST LATTICE PLANE - EFFECT ON SURFACE ENERGY

For purposes of the present work, attention was focused on Al, in which the lattice terms $\delta\sigma_{c1}$ and $\delta\sigma_{ps}$ are large.[41] The first plane of ions at the (111) face of the semi-infinite ($x < 0$) fcc structure was allowed to shift its position from $x = -\frac{1}{2}d$ to $x = (-\frac{1}{2} + \lambda)d \equiv x_\lambda$ (cf. Fig. 5), changing the surface energy by an amount $\Delta\sigma$. It is convenient to write

$$\Delta\sigma = \Delta\sigma_{c1} + \Delta\sigma_{ps} \quad ,$$

with the two terms corresponding to steps 1 and 2 of Fig. 5. Zero point motion of the ions will be neglected in computing these two contributions.

It may be seen using the analysis of Appendix D that $\Delta\sigma_{ps} = R(\lambda) - R(0)$, with

$$R(\lambda) = 4\pi d\bar{n}\int_{-\infty}^{x_\lambda - r_c}(x_\lambda - x)[n(x) - \bar{n}]dx + 2\pi d\bar{n}\int_{x_\lambda - r_c}^{x_\lambda + r_c}(x_\lambda + r_c - x)[n(x) - \bar{n}]dx \, . \tag{E1}$$

The pseudopotential cores are assumed here always to be to the left of the point $x = 0$ (i.e., $x_\lambda + r_c < 0$).

For the (111) face of the fcc lattice, use of techniques similar to those of Appendix C (with $\gamma \to \infty$ for simplicity) leads to the result $\Delta\sigma_{c1} = S(\lambda) - S(0)$, with

$$S(\lambda) = 2\pi\bar{n}^2\lambda^2 d^3 + \tfrac{1}{3}\sqrt{2}Z\bar{n}\sum_{l=0}^{\infty}\sum_{\mu=1}^{6}{}'\sum_{mn}{}'(m^2 + \tfrac{1}{3}n^2)^{-1/2} \times \cos(2m\pi b_\mu)\cos(2n\pi c_\mu) \times \exp[-2\pi(\sqrt{6})(l + a_\mu(\lambda))(m^2 + \tfrac{1}{3}n^2)^{1/2}], \tag{E2}$$

where the prime on $\sum_{mn}$ indicates omission of the term $m = n = 0$ and that on $\sum_\mu$ indicates omission of the terms $\mu = 1, 2$ when $l = 0$. Here $a_\mu(\lambda) = a_\mu + \frac{1}{3}\lambda$, with $a_1 = a_2 = 0$, $a_3 = a_4 = \frac{1}{3}$, and $a_5 = a_6 = \frac{2}{3}$; $b_{2n+1} = 0$, $b_{2n} = \frac{1}{2}$; and $c_{2n} = \frac{1}{3}n + \frac{1}{6}$, $c_{2n+1} = \frac{1}{3}n$. The first term in (E2) gives the energy change due to movement of the first lattice plane in the potential of the slab of negative charge between $x = -d$ and $x = 0$, and the second term gives the effect of the remainder of the crystal (which is neutral).

Minimization of $\Delta\sigma$ with respect to $\lambda$ showed the equilibrium interplanar distance at the surface to be only 0.5% larger than that of the bulk, with a reduction of $\sigma$ by just 2%. These results may be contrasted with those of Benson's analogous calculation for alkali halides.[42]

---

*Work supported in part by the National Science Foundation and the Office of Naval Research.

†Present address: IBM Watson Laboratory, Columbia University, New York, New York 10025.

[1]W. A. Harrison, *Pseudopotentials in the Theory of Metals* (Benjamin, New York, 1966).

[2]T. M. Rice, Phys. Rev. 175, 858 (1968).

[3]N. W. Ashcroft and D. C. Langreth, Phys. Rev. 155, 682 (1967).

[4]J. Frenkel, Z. Physik 51, 232 (1928).

[5]J. Bardeen, Phys. Rev. 49, 653 (1936).

[6]Reviews of theoretical work include C. Herring, in *Metal Interfaces* (American Society for Metals, Cleveland, 1952), p. 1; P. P. Ewald and H. J. Juretschke, in *Structure and Properties of Solid Surfaces*, edited by R. Gomer and C. S. Smith (University of Chicago Press, Chicago, 1953), p. 82; J. R. Smith, Phys. Rev. 181, 522 (1969).

[7]P. Hohenberg and W. Kohn, Phys. Rev. 136, B864 (1964).

[8]W. Kohn and L. J. Sham, Phys. Rev. 140, A1133 (1965).

[9]A. J. Bennett and C. B. Duke, in *Structure and Chemistry of Solid Surfaces*, edited by G. A. Somorjai (Wiley, New York, 1969).

[10]J. R. Smith, Ref. 6.

[11]N. D. Lang, Solid State Commun. 7, 1047 (1969).

[12]Results for the work function in this model have been reported in Ref. 11.

[13]B. Mrowka and A. Recknagel, Physik Zeits. 38, 758 (1937).

[14]A. Samoilovich, Acta Physicochim. URSS 20, 97 (1945).

[15]We use atomic units, with $|e|=m=\hbar=1$. In this system, the unit of energy is 27.2 eV.

[16]Equation (2.8a) can be understood in the following way. The chemical potential of a metal with a surface is the additional energy associated with adding an electron in its interior. This is the same as for an infinite metal, except for the difference in the electrostatic potentials existing in the interior. In the infinite uniform background model, this electrostatic potential is conventionally taken to be zero, and so (2.8a) follows.

[17]Equation (2.9), for the purposes of the present paper, may be simply regarded as the definition of the quantity $\Phi$. The proof that $\Phi$ is in fact the work function, including all many-body effects such as the image force, will be given in a later publication dealing with the work function.

[18]B. Y. Tong and L. J. Sham, Phys. Rev. 144, 1 (1966).

[19]E. P. Wigner, Phys. Rev. 46, 1002 (1934).

[20]K. S. Singwi, M. P. Tosi, R. H. Land, and A. Sjölander, Phys. Rev. 176, 589 (1968).

[21]J. Bardeen, Phys. Rev. 58, 727 (1940).

[22]Note that $\varphi$ is the negative of the total electrostatic potential. It differs from the $\varphi$ used earlier by an immaterial constant, which does not affect the value of (2.19).

[23]H. B. Huntington, Phys. Rev. 81, 1035 (1951). A factor $\pi^{-2}$ is omitted in Eq. (5) of this paper. See also R. Stratton, Phil. Mag. 44, 1236 (1953).

[24]Al: E. S. Levin, G. D. Ayushina, and P. V. Gel'd, Teplofizika Vysokikh Temperatur 6, 432 (1968) [High Temp. USSR 6, 416 (1968)]. Zn: D. W. G. White, Trans. Met. Soc. AIME 236, 796 (1966). Mg, Li: J. Bohdansky and H. E. J. Schins, J. Inorg. Nucl. Chem. 30, 2331 (1968); 29, 2173 (1967). Na, K, Rb, Cs: D. Germer and H. Mayer, Z. Physik 210, 391 (1968).

[25]The importance of treating the ions in metals as discrete in computing surface energies has been noted by S. N. Zadumkin, Fiz. Metal. i Metalloved. 11, 3 (1961); 11, 331 (1961) [Phys. Metals Metallog. 11, 3 (1961); 11, 11 (1961)].

[26]Calculations for bulk metals by N. W. Ashcroft and D. C. Langreth (Ref. 3) show that the first-order perturbation energy gives a very accurate description of the effects of the pseudopotentials.

[27]N. W. Ashcroft, Phys. Letters 23, 48 (1966).

[28]A correction would be necessary if the cleavage plane passed through an ion core ($r \leq r_c$ region). This does not occur in our calculations.

[29]See, for example, A. F. Skryshevskii and V. K. Grigorovich, in *Structure and Properties of Liquid Metals*, edited by A. M. Samarin (Academy of Sciences, Moscow, 1960).

[30]A. S. Skapski, Acta Met. 4, 576 (1956); C. Herring, Ref. 6.

[31]As noted earlier, these values represent linear extrapolations to zero temperature of the data of Ref. 24. The experimental surface tension is generally found to vary linearly above the melting point; but of course extrapolation to zero temperature is a very crude approximation. Use of simple theories for the temperature dependence of $\sigma$, however, give results that (except for Zn) agree roughly with this procedure [see K. Huang and G. Wyllie, Proc. Phys. Soc. (London) A62, 180 (1949)].

[32]See discussion in D. W. G. White, Ref. 24.

[33]The use of an $r_c$ value obtained from the condition $\partial E/\partial r_s = 0$ (as in Ref. 3), with $E$ the bulk energy, changes the calculated $\sigma$ values substantially only in the cases of Zn (an increase of 200 ergs/cm$^2$ – cf. other experimental values quoted in D. W. G. White, Ref. 24) and Pb (a decrease of 220 ergs/cm$^2$ – see next paragraph).

[34]D. A. Melford and T. P. Hoar, J. Inst. Metals 85, 197 (1956).

[35]For the metals considered, the entire zero point energy of a bulk atom is, for one degree of freedom, only of the order of 5% of the surface energy per atom. This supports our assumption that vibrational effects make only minor contributions to their surface energies.

[36]W. Kohn and L. J. Sham, Phys. Rev. 137, A1697 (1965).

[37]R. D. Misra, Proc. Cambridge Phil. Soc. 36, 173 (1940).

[38]B. M. E. van der Hoff and G. C. Benson, Can. J. Phys. 31, 1087 (1953).
[39]R. A. Coldwell-Horsfall and A. A. Maradudin, J. Math. Phys. 1, 395 (1960).
[40]E. T. Whittaker and G. N. Watson, *A Course of Modern Analysis* (Cambridge U.P., Cambridge, 1927), 4th ed., p. 474.
[41]The $r_s$ value which minimized the total energy of the solid was employed in this calculation. Equation (5) of Ref. 3, exclusive of second-order terms, with Wigner's form for the correlation energy (Ref. 19), was used to obtain this $r_s$ (which was 2.10 for Al).
[42]G. C. Benson, J. Chem. Phys. 35, 2113 (1961).

PHYSICAL REVIEW B VOLUME 1, NUMBER 12 15 JUNE 1970

# Ionized-Impurity-Limited Mobility of α-Sn in the Random-Phase Approximation*

J.G. Broerman

*McDonnell Research Laboratories, McDonnell Douglas Corporation, St. Louis, Missouri* 63166
(Received 29 January 1970)

A calculation of the ionized-impurity-limited mobility of a $\Gamma_8$ conduction band is performed, using a random-phase-approximation dielectric function and taking into account the effects of band nonparabolicity and $p$-like character of the wave function on the scattering calculation. The results are compared with measured mobilities of Sb-doped α-Sn. It is shown that, assuming singly ionized donor impurities, the calculated results are grossly larger than the experimental values. The results are somewhat better for doubly ionized impurities. It is pointed out that the results of a calculation using a concentration-independent dielectric constant are in excellent agreement with experiment over the whole range of accessible concentration. These results indicate that, if the impurities are singly ionized Sb, the random-phase approximation considerably overestimates the interband polarization.

## I. INTRODUCTION

α-Sn is the allotrope of tin with the diamond crystal structure. Its electron band structure is similar to that of other diamond structure members of column IV, except that the $s_{1/2}$-like $\Gamma_6^-$ level is depressed so as to lie between the $p_{3/2}$-like $\Gamma_8^+$ level and the $p_{1/2}$-like $\Gamma_7^+$ level.[1] Part of the fourfold-degenerate $\Gamma_8^+$ band then becomes a conduction band and part a valence band. The closest lying band extremum, $L_6^+$, lies slightly above $\Gamma_8^+$, and thus the material becomes a perfect semimetal with a symmetry-induced degeneracy of the valence-band maximum and conduction-band minimum. For this reason, it has been the subject of considerable interest as a candidate for an excitonic phase transition.

However, Liu and Brust,[2] using the random-phase approximation, showed that, because the degeneracy of the band edges is symmetry induced, the static dielectric function $\epsilon(q)$ diverges like $q^{-1}$ as $q \to 0$. The presence of impurity carriers is sufficient to remove this divergence through Thomas-Fermi screening, leaving a finite interband part which is strongly dependent on impurity carrier concentration. Liu and Tosatti[3] calculated the concentration-dependent dielectric function in the random-phase approximation and showed that the resulting ionized-impurity-limited mobilities were in excellent agreement with the anomalously large values[4,5] observed in degenerate $n$-type samples.

Liu and Tosatti, in their scattering calculation, treated the conduction electrons as $s$-like with a parabolic dispersion relation. However, α-Sn conduction electrons are $p$-like, and there are considerable differences between the scattering cross sections of $s$- and $p$-like electrons.[6] Differential scattering cross sections for large-angle scattering of $p$-like electrons are much smaller than those for $s$-like electrons. This is especially important in a mobility calculation because the Boltzmann equation heavily weights large-angle scattering. In addition, the α-Sn conduction-band dispersion relation is quite nonparabolic, the effective mass at the Fermi surface changing by 30% in the concentration range considered by Liu and Tosatti. Since the density of states enters the mobility calculation squared, the nonparabolicity is quite important. A calculation was performed[7] which showed that excellent agreement could be obtained with the observed mobilities,[4,5] using a concentration-independent background dielectric constant and taking into account the $p$-like character of the wave function and the nonparabolicity of the conduction-band dispersion relation.